UNIVERSITY OF BIRMINGHAM

University of Birmingham Research at Birmingham

Prediction of the knock propensity of biogenous fuel gases

Lechner, Raphael; Hornung, Andreas; Brautsch, Markus

[Link to publication on Research at Birmingham portal](#)

Prediction of the knock propensity of biogenous fuel gases: Application of the detonation theory to syngas blends

Lechner, R.[a,d,*], Hornung, A.[a,b,c], Brautsch, M.[d]

[a] University of Birmingham, School of Chemical Engineering, Edgbaston, Birmingham B15 2TT, United Kingdom

[b] Friedrich-Alexander University Erlangen-Nürnberg, Department of Chemical and Biological Engineering, Immerwahrstraße 2a, 91058 Erlangen, Germany

[c] Fraunhofer UMSICHT, An der Maxhütte 1, 92237 Sulzbach-Rosenberg, Germany

[d] OTH Amberg-Weiden – Technical University of Applied Sciences, Centre of Excellence for Cogeneration Technologies, Kaiser-Wilhelm-Ring 23, 92224 Amberg, Germany

*Corresponding Author: r.lechner@oth-aw.de

Abstract:

Prediction of the knock propensity is crucial for design and control of engines operating on syngas from thermo-chemical conversion. Classical fuel rating methods such as the methane number or the propane knock index were found to fail for the syngas compositions encountered in practice. A detailed chemical kinetics simulation of the critical compression ratio in an ideal homogenous auto-ignition reactor was tested as an alternative rating method, but was found to also have serious drawbacks and provoke misleading results due to overlying thermodynamic effects. Thus, a novel methodology based on the detonation theory was successfully adopted. The method centres on the two dimensionless parameters ξ and ε which characterise the possible regimes of auto-ignition propagation originating from hot spots. The ξ-ε diagram was applied to a total of 38 fuel blends including reference fuels and syngas compositions determined with a statistical mixture plan supplemented by measured data. The gas measurements were taken at an industrial scale intermediate pyrolysis plant featuring the Thermo-Catalytic Reforming technology of Fraunhofer UMSICHT. Practically all syngas blends showed to be more prone to knock than methane or biogas, albeit not more than propane, which is a standard fuel used in gas engines. Admixtures of higher hydrocarbons were found to substantially increase the knock propensity. Lean equivalence ratios, exhaust gas recirculation and the addition of water vapour were effective measures to mitigate the risk of knock. The anti-knock effect of dilution could be primarily attributed to a reduction of the amount of energy transferred into the acoustic front of an auto-ignition wave.

Keywords: syngas, knock, prediction, methane number, detonation theory, Thermo-Catalytic Reforming

Symbols

a	Acoustic velocity	m/s
CR_c	Critical compression ratio	-
c_p	Specific heat capacity at constant pressure	J/(kg K)
c_v	Specific heat capacity at constant pressure	J/(kg K)
E	Activation energy	J/mol
$\bar{E}$	Dimensionless parameter $\bar{E} = \tau_i/\tau_e \cdot E/(RT)$	-
E/R	Activation temperature	K
P	Pressure	Pa
R	Universal gas constant	J/(mol K)
r	Radius	m
r_0	Hot spot radius	m
$\bar{r}$	Dimensionless hot spot radius $\bar{r} = r/r_0$	-
T	Temperature	K
T_0	Temperature at centre of hot spot	K
u_p	Auto-ignitive propagation speed	m/s
ε	Dimensionless parameter $\varepsilon = r_0/(a/\tau_e)$	-
ξ	Dimensionless parameter $\xi = a/u_p$	-
ρ	Density	kg/m³
τ_i	Ignition delay time	s
τ_e	Excitation time	s
ϕ	Fuel/air equivalence ratio	-

Abbreviations

C	Carbon
CFR	Cooperative Fuel Research
C_xH_y	Generic higher hydrocarbon
DoE	Design of Experiments
EGR	Exhaust gas recirculation
GRI	Gas Research Institute
H	Hydrogen
HCCI	Homogenous charge compression ignition
HHV	Higher heating value
LHV	Lower heating value
MN	Methane number
N	Nitrogen
O	Oxygen
PKI	Propane knock index
TCR	Thermo-Catalytic Reforming
vol%	Volume percent
wt%	Weight percent

1.   Introduction

Thermo-chemical conversion and particularly intermediate pyrolysis is a promising technology to convert biomass residues into valuable fuels, namely bio-oil, char and permanent gases. The gas fraction – which is also known as syngas – is particularly interesting for the use in stationary internal combustion engines. In practice, the composition of the permanent gases from thermo-chemical conversion can vary considerably according to the feedstock and the process settings. A compilation of reported gas qualities from different sources is presented in Table 1.

While the loss of power production due to the lower heating values of syngas blends is readily understood and can be compensated for, the knock-resistance is the decisive parameter that can limit the usability of fuel gases in engines [1]. Admixtures of higher hydrocarbons are especially challenging with regard to knock in natural gas fuelled engines [2] and it can be expected that this is also the case with syngas blends.

The classical method for assessing the knock propensity of gaseous fuels is the methane number which was originally developed by the company AVL in the 1960s based on experimental data from a test engine with variable compression ratio [3,4]. For the determination of the methane number the compression ratio of the engine is continually increased until knock is detected at the critical compression ratio (CR_c). The test is then repeated with variable mixtures of methane and hydrogen keeping the identified critical compression ratio constant and increasing the hydrogen content until knock is detected again. The obtained mixture of methane and hydrogen defines the methane number, with hydrogen being equivalent to MN = 0 and methane being equivalent to MN = 100. For gases with even higher knock resistance CO_2 is added on top, resulting in methane numbers > 100 [3].

However, the methane number has shortcomings, especially for blends with high shares of H_2 and at the same time CO [1] and for gases containing higher hydrocarbons with methane numbers less than approximately 50 [2]. Furthermore, it was developed from a specific test engine operating under stoichiometric conditions and it is discussed if the method is still suitable for the actual diversity of engine designs and modern machines, that tend to operate under fuel-lean conditions and at higher pressures [5]. It this thus necessary to develop new methods for assessing the knock propensity of non-conventional fuel gases.

Van Essen et al. [5,6] developed such a new knock characterisation method for fuel gases based on the auto-ignition delay time in the compressed end gas which is determined with the help of a two-zone thermodynamic model using detailed chemical kinetics. The model was derived from experimental tests on a 6-cylinder gas engine applying mixtures of CH_4 and Dutch natural gas with H_2, CO and higher hydrocarbons, such as ethane and propane, iso-butane and n-butane. A ranking tool was constructed, in which a mixture of methane and propane which exhibits the same simulated auto-ignition behaviour as the test gas serves as a benchmark. The obtained result is the propane knock index (PKI). An online calculator for the PKI is available from DNV GL [7].

A similar approach is followed by Schultze et al. [8] who experimentally and numerically investigated the utilisation of hydrogen-rich fuel gases in large gas engines. Schultze applied a piston reactor model – which reproduces an ideal homogenous charge compression ignition (HCCI) – for modelling auto-ignition. The reactor is referred to as rapid compression machine model by the authors. They used the Cantera code [10] for simulation and applied the GRI-Mech 3.0 kinetic mechanism [9] as well as their own modification of the mechanism optimised for H_2 and CO-rich fuel gases. The piston reactor model was found to be suitable for qualitative predictions of knock-resistance, although the trends of the experimental results could not be reproduced in all

3

cases. Still, the authors consider the model to be a better approach than the methane number for gases with high contents of H_2 and at the same time CO.

Wise [1] studied the utilisation of producer gas from biomass gasification in high performance natural gas engines both experimentally and numerically, using a Cooperative Fuel Research (CFR) F-2 fuel research engine and applying a chemical kinetics simulation with CHEMKIN. Wise investigated a total of 35 different blends based on real producer gas compositions encountered in practice, and experimentally determined both the critical compression ratio at the onset of knock as well as the methane number of a the corresponding blend of CH_4 and H_2. In some cases the experimental results differed considerably (up to 30 units, average 11.1 units) from the calculated methane numbers according to the AVL method, with the largest over prediction occurring for blends with large CO and H_2 content and very little methane content. Wise implemented a (HCCI) reactor model to predict the methane number numerically, using detailed chemical kinetics to model auto-ignition. However, the simulation results were not consistent with the experimental measurements. According to Wise this is due to the fact that the HCCI model does not consider flame propagation as it occurs in real engines. Nonetheless, Wise concludes that the methane number is a fuel property that could be ascertained solely through knowledge of the constituent make-up of the fuel.

Building upon the work of Wise, Montoya et al. [11] investigated the methane number and critical compression ratio of twelve biogas blends with methane, propane and hydrogen. They used the same experimental setup and HCCI reactor simulation as Wise, but applied several different reaction mechanisms in order to identify the most suitable for the given fuel blend. It was, however, not possible to find an optimal mechanism for all gaseous blends to reproduce both the critical compression ratio and the methane number.

A different approach is followed by Bates et al. [12] who applied the detonation theory by Bradley et.al. (cf. [13]) for assessing the knock propensity of stoichiometric mixtures of methane/air. According to the detonation theory the evolution of an auto-ignition event from a hot spot can be described using two dimensionless parameters ξ and ε [14]. The parameter ξ relates the speed of sound a to the auto-ignition propagation velocity u_p. If the two velocities are of the same magnitude the auto-ignition wave and the acoustic wave can reinforce each other and grow to a developing detonation leading to engine knock [14]. In case that the reaction velocity is much slower than the acoustic velocity the subsonic auto-ignition regime is entered which is not harmful for the engine [14]. If the opposite is true and the reaction wave travels ahead of the acoustic wave the regime of supersonic auto-ignitive deflagration will be entered resulting in a thermal explosion at $\xi = 1$ (cf. [15]). The second parameter ε is used to determine the amount of energy transferred to the acoustic wave during the time it travels through the hot spot. Together, the two parameters confine a detonation peninsula in which harmful knock can develop. Both ξ and ε can be determined by chemical kinetic simulations without the need for experimentation. Thus, the detonation theory has the potential to be used as a method for the a priori assessment of the knock propensity of fuels based solely on their constituents. It can also be applied for predicting knock at specific engine operating points, as recently shown by Netzer et al. [14], who successfully used the ξ-ε diagram with a three-dimensional computational fluid dynamics analysis to predict knocking regimes in a gasoline-fuelled passenger car engine.

Based on the current state of knowledge there is still no reliable method for a priori assessing the knock propensity of complex syngas compositions as they occur in practical application. Thus, the aims of this paper are

- to determine a representative range of fuel compositions from thermo-chemical conversion as occurring in practice,
- to investigate whether the methane number or other knock indexes, such as the PKI knock index and alternative approaches such as the HCCI simulation of auto-ignition are applicable to assess the knock propensity of these fuels,
- to adopt the novel method of the ξ-ε diagram to assess the knock propensity of syngas blends,
- to investigate the effects of exhaust gas recirculation and water vapour with regard to mitigation of knock-risk by means of the ξ-ε diagram.

This is the first time the detonation theory is applied to practical syngas compositions and the first time that the effects of different equivalence ratios, EGR and water vapour are also considered.

Table 1: Intermediate pyrolysis gas composition from different feedstocks and processes

Source	Process / feedstock / post reforming temperature [a] / gas yield	Heating value [b]	H_2	CO	CH_4	CO_2	N_2	C_xH_y	Not detected / others
			vol%	vol%	vol%	vol%	vol%	vol%	vol%
Conti [16]	TCR / wood chips / 973 K / 62.7 wt%	-	24.0	22.0	12.0	22.0	-	2.0	18.0
	TCR / digestate / 973 K / 31.7 wt%	-	33.0	16.0	8.0	23.0	-	2.0	18.0
	TCR / sewage sludge / 973 K / 18.5 wt%	-	38.0	12.0	3.0	15.0	-	3.0	29.0
	TCR / paper sludge / 973 K / 19.1 wt%	-	40.0	10.0	1.0	27.0	-	3.0	19.0
Neumann [17]	TCR / digestate / - / 18 wt%	LHV 9.7 MJ/m³	7.0	43.0	6.0	40.0	-	-	4.0
	TCR / digestate / 773K / 20 wt%	LHV 13.1 MJ/m³	21.0	14.0	5.0	40.0	-	-	20.0
	TCR / digestate / 1 023K / 35 wt%	LHV 14.4 MJ/m³	37.0	12.0	3.0	28.0	-	-	20.0
Jäger [18]	TCR / vine shoots / 973 K / 57 wt%	-	36.0	15	10.0	27.0	-	1.5	10.5
	TCR / evergreen oak / 973 K / 58 wt%	-	36.0	16.0	12.0	27.0	-	1.0	8
	TCR / olive tree / 973 K / 60 wt%	-	33.0	16.0	12.0	27.0	-	1.5	10.5
Mahmood [19]	Pyroformer / brewers spent grain / - / 33-34 wt%	1-2 MJ/m³	1.6	19.7	9.4	64.2	4.6	-	O_2 0.45
Ouadi [20]	Pyroformer / de-inking sludge 1 /- / -	HHV 5.5 MJ/m³	0.0	22.7	6.1	71.2	-	-	-
	Pyroformer / de-inking sludge 2 /- / -	HHV 6.2 MJ/m³	1.9	25.5	6.3	66.3	-	-	-
Yang [21]	Pyroformer / wood pellets / - / 17.7 wt%	HHV 7.27 MJ/m³	2.2	34.7	7,2	50.3	5.5	-	-
	Pyroformer / barley straw /- / 20.9 wt%	HHV 6.92 MJ/m³	1.5	21.7	10.5	60.1	4.7	-	O_2 0.42

[a] if applicable, [b] as reported, [c] pyrolysis temperature
LHV: lower heating value; HHV: higher heating value

2. Methodology

Investigated fuel gases

Since the composition of biogenous fuel gases from thermo-chemical conversion can vary considerably, a thorough assessment of the combustion characteristics must cover a wide range of fuel compositions. Thus, a statistical *design of experiments (DoE)* was used to define a fuel matrix covering the relevant range of fuel compositions from different gasification and intermediate pyrolysis technologies with different feedstocks. The software tool Cornerstone by camLine (version 7.1 http://www.camline.com) was used for this purpose. Based on a review of published fuel data from 16 studies (including the data presented in Table 1) a mixture plan covering 31 gas mixtures was developed using a D-optimal statistical design. The gas mixtures were assumed to consist of H_2, CO, CH_4, CO_2, and higher hydrocarbons up to C3. N_2 was used as filler to complete the mixture. C_2H_4, C_2H_6 and C_3H_8 were selected as representatives of higher hydrocarbons based on the reported data. Additionally, pure methane, pure propane, pure hydrogen and a biogas mixture consisting of 60 vol% CH_4 and 40 vol% CO_2 were examined as reference fuels.

In order to supplement the data from literature, pyrolysis gas measurements were performed at an industrial scale TCR® pyrolysis plant using a micro gas chromatograph of type Agilent 490. Thermo-Catalytic Reforming (TCR®) is an intermediate pyrolysis process developed by Fraunhofer UMSICHT capable of operating on a wide range of residue biomass feedstocks. The TCR reactor is a multi-zone auger reactor with different zones through which the feedstock is transported by a screw conveyor while being heated using a specific temperature profile [22]. In the auger reactor, pyrolysis and a first reforming step take place at temperatures of about 623 K to 723 K with residence times from 5 to 10 min [23]. The resulting intermediates are then conveyed into a post-reformer, where the organic fraction is catalytically reformed at a maximum temperature of 1 023 K [23] resulting in an essential upgrade of all phases [22]. A schematic of the process is presented in Figure 1.
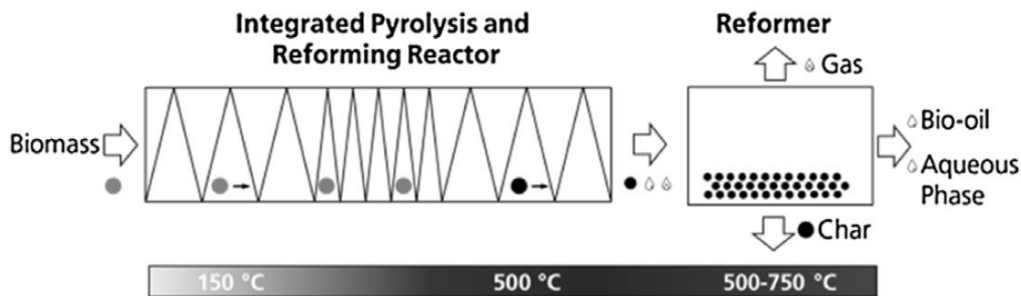

Figure 1: Schematic of the TCR process [22]

Table 2: Investigated fuel gas blends

#	H$_2$ vol%	CO vol%	CH$_4$ vol%	CO$_2$ vol%	C$_2$H$_4$ vol%	C$_2$H$_6$ vol%	C$_3$H$_8$ vol%	C$_x$H$_y$ vol%	N$_2$ vol%
1	15	50	15	10		5	5		
2	40	30	7.5	10		3.75	2.5		6.25
3		50		45	5				
4		32.5	7.5	50	2.5	2.5	5		
5	40	25	15	10	5		5		
6	10	10	15	40	2.5	2.5			20
7	20	10	15	50	2.5		2.5		
8	20	50		10		1.25			18.75
9	15	50	15	10	5				5
10	15.74	29.26	15	10	2.5	5	2.5		20
11		50		40		5	5		
12	40	10		20		5	5		20
13	40	30		20	5	5			
14	20	10		50	5	2.5	2.5		10
15	15	50		10	5		5		15
16	25	10		50		5			10
17		20	15	50	5	5			5
18	20	50	5	22.5			2.5		
19	5	10	15	40	5		5		20
20	40	10	15	20	5	5			5
21	40	25	15	20					
22	40	10		25	5				20
23	35	10		50			5		
24	5	10	15	50		5	5		10
25		50	5	15	5	5			20
26		30	11.25	50					8.75
27		50	15	25	5	2.5	2.5		
28		50	15	10			5		20
29	20	20	15	30		2.5	5		7.5
30		50	15	30		5			
31		35		40			5		20
32			100						
33			60	40					
34							100		
35	100								
36	16.75	19.85	13.81	15.67	1.73	1.16	0.35	2.45[a]	28.23
37	16.75	19.85	13.81	15.67	1.73	1.16	0.35	2.45[b]	28.23
38	16.75	19.85	13.81	15.67	1.73	1.16	0.35	0.09[c]	30.59

a) iso-C$_4$H$_{10}$ 0.09 vol%, n-C$_7$H$_{16}$ 2.36 vol%
b) iso-C$_4$H$_{10}$ 0.09 vol%, iso-C$_8$H$_{18}$ 2.36 vol%
c) iso-C$_4$H$_{10}$ 0.09 vol%

Including the fuels defined in the DoE plan, the reference fuels and the measured TCR gas compositions, a total of 38 fuel gases were investigated (cf. Table 2). In order to simplify the nomenclature the gas compositions #1 to #31 will henceforth be identified as *syngas* blends. *Biogas* (blend #33) will be referred to with its full name and *methane* (blend #32), *propane* (blend #34) and *hydrogen* (blend #35) will be referred to with their full name or their chemical symbol for better readability in graphs. The measured pyrolysis gas compositions from the TCR® pilot plant (blend #36 to #38) will be denominated *TCR gas* for differentiation.

In case of the TCR gas iso-butane (0.09 vol%) and higher hydrocarbons C5+ (2.36 vol%) were detected in the blend (cf. Table 2 blend #36 to #38). Apart from iso-pentane at about 0.03 vol% the exact composition of the C5+ fraction could not be resolved. Thus, three scenarios were defined using primary reference fuels as representatives of higher hydrocarbons:

 a) a "knock-prone" C5+ fraction represented by n-heptane
 b) a "knock-resistant" C5+ fraction represented by iso-octane
 c) the C5+ fraction set to zero and replaced by nitrogen (no C5+ hydrocarbons in the fuel)

Determination of the methane number

The methane numbers of the investigated fuels were determined according to the MWM method with the computer program available from EUROMOT [24]. In about half of the cases, the calculator issued a confidence warning for the methane number and in one case (fuel #25), the calculation failed completely. Thus, the Cummins Westport Fuel Quality Calculator [25] and the DNV Propane Knock Index calculator tool [7] were applied additionally. However, none of these tools was able to handle the provided gas compositions, since C_2H_4 is not supported as constituent and either H_2, CO, CH_4 or CO_2 were outside the range of validity.

HCCI reactor simulation

Following Wise [1] and Montoya [11] a HCCI reactor simulation with detailed chemical kinetics was set up for the determination of the critical compression ratio. The geometry of a CFR F-2 fuel research engine was assumed for the reactor and the initial conditions and the rotational speed were set to the operating conditions of the motor octane number test (cf. Wang [26]). Stoichiometric and lean mixtures were investigated accordingly. The evaluated crank angle range was 360° with a resolution of 0.05° and the compression ratio was automatically adjusted until auto-ignition at the top dead centre (180° crank angle) occurred. The according compression ratio was taken as the critical compression ratio CR_c. Heat transfer and gas exchange with the surroundings were not considered (closed adiabatic reactor). A summary of the simulation settings is given inTable 3.

Table 3: HCCI reactor simulation settings for determining CR_c

Parameter	Value
Bore	8.255 cm
Stroke	11.43 cm
Displacement	611.7 cm³
Ratio connecting rod length to crank radius	4.44
Rotational speed	900 1/min
Initial pressure	0.1 MPa
Initial mixture temperature	422 K
Equivalence ratio	1.0, 0.5
Evaluated crank angle range / resolution	360° / 0.05°
Auto-ignition crank angle	180° (top dead centre)
Heat transfer	adiabatic

Determination of the parameters ξ and ε.

The dimensionless parameters *ξ* and *ε* were determined following the methodology presented by Bates et al. [27]. The parameter *ξ* relates the acoustic velocity *a* to the auto-ignition propagation velocity u_p:

$$\xi = \frac{a}{u_p} \tag{1}$$

The auto-ignition propagation velocity is equal to the inverse gradient of the auto-ignition delay time

$$u_p{}^{-1} = \left(\frac{\partial \tau_i}{\partial r}\right) \tag{2}$$

which can be decomposed into a product of the thermal gradient $\partial T/\partial r$ throughout the auto-ignition hot spot and the thermal sensitivity $\partial \tau_i / \partial T$ yielding:

$$\xi = \frac{a}{u_p} = \frac{\partial T}{\partial r}\frac{\partial \tau_i}{\partial T} a \tag{3}$$

By introducing the thermal sensitivity of the ignition delay time

$$\frac{\partial \tau_i}{\partial T} = -\tau_i \frac{E}{RT^2} \tag{4}$$

Equation (3) can be rearranged to:

$$\xi = -\tau_i \frac{E}{RT^2} \frac{\partial T}{\partial r} a \tag{5}$$

The ignition delay time τ_i and the activation temperature *E/R* can be determined by chemical kinetics simulations. The acoustic velocity for an ideal gas mixture can be obtained from:

$$a = \sqrt{\frac{c_p}{c_v} \frac{P}{\rho}}$$ (6)

where c_p and c_v are the heat capacities at constant pressure and volume, P is the pressure and ρ is the density.

The second dimensionless parameter ε represents the amount of energy transferred to the acoustic wave during the time it travels through the hot spot of radius r_0:

$$\varepsilon = \frac{r_0}{a\tau_e}$$ (7)

The excitation time τ_e is determined by the heat release during the auto-ignition event and is defined as the time span between the point where 5 % of the maximum heat release rate is reached and the point where the maximum is attained (cf. Figure 2 and definition given by Bates in [12]).

The product ξ times ε yields a dimensionless parameter group introduced by Bates [27] to distinguish between the regimes of deflagration and subsonic auto-ignition:

$$\xi\varepsilon = -\bar{E}\left(\frac{\partial lnT}{\partial \bar{r}}\right)$$ (8)

$$\bar{E} = \frac{\tau_i}{\tau_e} \frac{E}{RT}$$ (9)

$$\bar{r} = \frac{r}{r_0}$$ (10)

where $\bar{r}$ is the dimensionless hot spot radius.

For qualitative assessment of fuels the hot spot radius and the temperature gradient can be approximated by $r_0 = 5$ mm and $\partial T / \partial r = -2$ K/mm (cf. [12]).

Chemical kinetics simulation

The Cantera [10] code implemented into an in-house Python environment was used as solver both for the HCCI reactor simulation and for the calculation of ignition delay and excitation times. The ignition delay time was determined with a homogenous, adiabatic constant-volume reactor model as the time span from the start of the simulation until the maximum of the heat release rate was detected. Adaptive time meshing with time steps down to 1×10^{-12} s in regions of high curvature was used. The activation temperature *E/R* was determined from a linear fit of the logarithmic ignition delay time over the inverse temperature (Arrhenius plot, cf. Figure 2). For exact determination of the excitation time the heat release curve was interpolated at its lower bound using cubic splines (cf. [12]).

Currently the only method to obtain excitation times is through numerical simulations [12]. Thus, the methodology is very sensitive with regard to the applied chemical kinetic mechanism. In this study the hierarchical comprehensive kinetic scheme developed at the Politecnico di Milano (cf. [28]) was used in a reduced version covering C1 to C3 fuels with high and low temperature chemistry. For the fuels containing hydrocarbons C4+ an extended version of the scheme covering also primary reference fuels and real fuels was used.
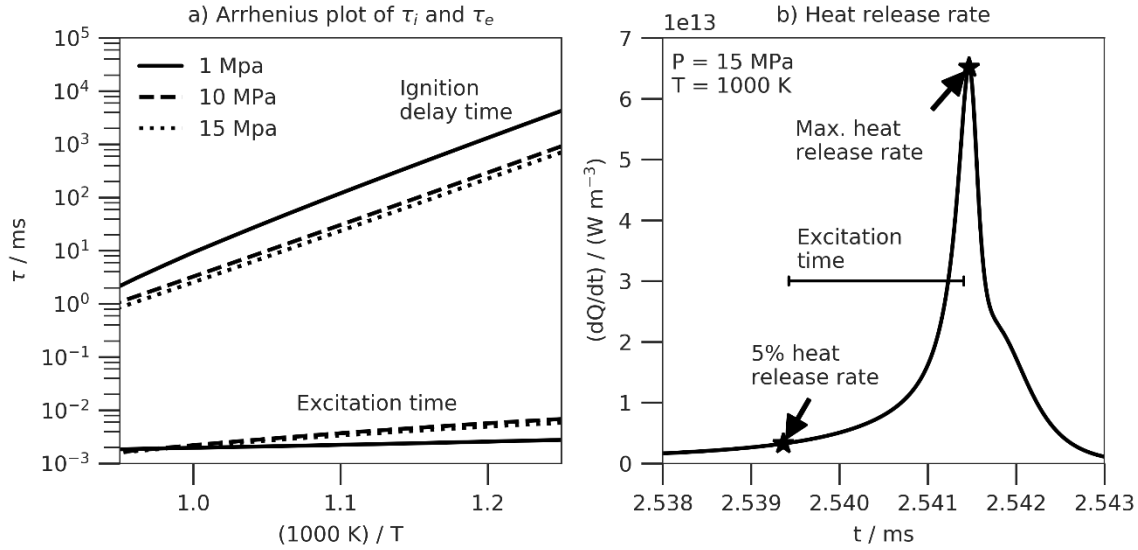
Figure 2: a) Arrhenius plot and b) heat release for combustion of H_2/CO/N_2 = 40/20/40 vol% at ϕ = 0.5

3.   Results and Discussion

HCCI reactor simulation

In Figure 3 the critical compression ratio CR_c obtained from the HCCI reactor simulations for the respective fuel is plotted against the MWM methane number obtained with the EUROMOT calculator for both stoichiometric (ϕ = 1) and lean (ϕ = 0.5) fuel-to-air equivalence ratios. The confident values for the methane number are marked with dots and the non-confident values are marked with crosses. When sorting out the values marked as non-confident by the EUROMOT calculation tool, a linear correlation between the MWM methane number and the critical compression ratio can be observed, although with considerable scatter. Due to the scatter a straightforward interpretation is not possible and certain fuels with almost identical methane number may exhibit very different values of CR_c.

The reference fuels biogas and CH_4 feature both high methane numbers and high values of CR_c, confirming their excellent resistance to knock. By comparison, most of the syngas blends and measured TCR gas blends generally exhibit lower values of CR_c, indicating that they are more prone to auto-ignition and probably knock.

As expected, the "knock-resistant" blend #37, which contains iso-octane as representative of higher hydrocarbons features a higher critical compression ratio than blend #36, to which n-heptane was added. It is interesting that blend #38, in which the C5+ hydrocarbons were replaced by nitrogen, has in fact a considerably higher methane number, as expected, but shows a slightly lower critical compression ratio than blend #37. A possible reason for this contradictory behaviour is that the fuel-air-mixture #38 has a higher heat capacity ratio (isentropic expansion coefficient) which implies that the temperature and pressure conditions required for auto-ignition are reached already at a lower compression ratio. The lower CR_c can thus be primarily attributed to thermodynamic effects rather than to the actual reactivity of the fuel.

11

The critical compression ratios of the lean mixtures are generally lower for most fuels with the exception of hydrogen. Again, this can be attributed mainly to the heat capacity ratio which is higher in case of the lean mixtures. The opposite is true for hydrogen.

It should be noted that a lower critical compression ratio does not necessarily imply a higher tendency to knock in the present context, since the HCCI reactor simulation reproduces a homogenous, strong auto-ignition rather than typical knock in the unburned end gas, which might explain some of the difficulties encountered when using the method as rating tool for the knock propensity of fuels (cf. [1,8,11]). It should also be considered that the methane number itself might not be an accurate measure for the knock propensity of syngas blends, since the method was developed primarily for natural gas and is not well defined for blends with high shares of hydrogen and carbon monoxide [1].
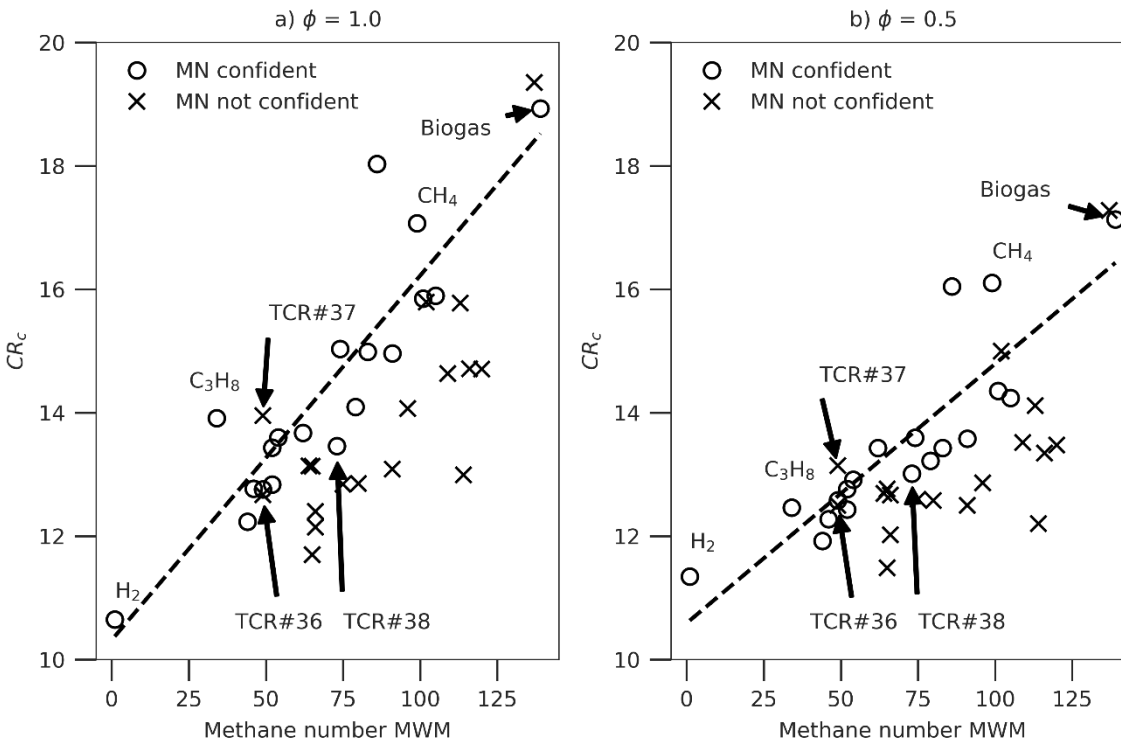

Figure 3: Critical compression ratio vs. methane number for stoichiometric and lean mixtures

Auto-ignition propensity in the ξ-ε diagram

In Figure 4 and Figure 5 the ξ-ε diagrams for the investigated fuels are shown for stoichiometric and lean equivalence ratios (observe the different scaling of the ε-axis). The detonation peninsula is marked with solid lines. Additionally, a transition regime between subsonic auto-ignition and deflagration which was tentatively defined by Bates [12] as $-\bar{E}(\partial lnT/\partial \bar{r}) \approx 900\ldots6\,000$ is marked with dashed lines.

The empty circles represent the approximate state at the end of an isentropic compression to 8 MPa and 800 K in a turbocharged, high speed, spark ignited gas engine with intercooler. The half-filled diamonds depict the state if this compression is continued to a pressure of 15 MPa at

≈ 950 K during combustion, assuming that the end gas core is adiabatic, that is, no heat is transferred from the flame to the unburned zone. Additionally, a state with identical pressure but at an elevated temperature of 1 100 K is displayed (half-filled triangles).

At stoichiometric conditions, 8 MPa and 800 K all fuel blends are within the safe operating regime of deflagration or in the transition region to subsonic auto-ignition. When the pressure and temperature are increased to 15 MPa and 950 K, the fuel isentropes move towards the upper limit of the detonation peninsula into the transition regime where auto-ignition and deflagration can coexist. While auto-ignitions in the subsonic regime are not harmful for the engine (cf. [14]) damaging knock may occur when entering the detonation peninsula. At 15 MPa and 950 K TCR blend #36 and propane are already in a regime where knock is to be expected. Finally, at the elevated temperature of 1 100 K, practically all fuels are well within the detonation peninsula approaching values of ξ close to unity which are associated with heavy knock and super-knock [27].

Altogether, methane and biogas show the highest resistance to knock, while propane and the TCR gas blends are generally more prone to knock. Hydrogen is not displayed in the ξ-ε diagram since it is located far to the right of the peninsula at values of $\varepsilon > 100$. Generally, values of $\varepsilon > 22$ (as occurring, e.g., for propane and methane) exceed the limits for which the detonation peninsula is currently defined. This limits the applicability of the ξ-ε diagram for fuels that feature very low excitation times. Additional work will thus be necessary to extend the current limits of the detonation peninsula towards larger values of ε. The same applies to the narrow open tip of the peninsula, which has to be further defined, particularly when considering fuels that exhibit very low values of ε and values of ξ being close to unity.

As opposed to the results from the HCCI reactor simulation the TCR gas blends #36 to #38 now show the expected behaviour with blend #38 (no C5+ hydrocarbons) being the most knock-resistant and blend #36 (n-heptane added) being most prone to knock. At 800 K and 8 MPa blend #36 is already in the region of subsonic auto-ignition near to the upper limit of the detonation peninsula. It is remarkable that even iso-octane – which is comparatively knock-resistant – increases the knock propensity considerably compared to blends without C5+ hydrocarbons (cf. TCR blend #37 vs. TCR blend #38). This indicates the prominent role of higher hydrocarbons with regard to the knock propensity of fuel gases.

When moving to lean equivalence ratios (Figure 5) the values of ε for all fuels decrease considerably. Most fuel blends are now in the safe operating regime of deflagration or subsonic auto-ignition and only enter the detonation peninsula at the elevated temperature of 1 100 K. The TCR fuel and propane blends are all within the narrow tip of the detonation peninsula at this temperature, with TCR #36 and propane approaching its lower limit, indicating that heavy knock and super-knock are probable for this fuels. It should be noted that the narrow open tip of the detonation peninsula is currently only loosely defined and may correspond to a regime where multiple modes of propagation may coexist [29]. Thus, in the present case this region should be simply interpreted as a condition where knock cannot be precluded.

It is remarkable that at lean equivalence ratios biogas does not enter the detonation peninsula at any conditions, not even at 15 MPa and 1 100 K. This corresponds very well with practical experience and confirms the excellent anti-knock characteristics of biogas. However, it is also noteworthy that practically all investigated syngas blends, including the TCR blends with higher hydrocarbons, are not more prone to knock than pure propane, which is a fuel commonly used in gas engines today (cf. liquefied petroleum gas). Thus, the utilisation of syngas as engine fuel should not present a major technical challenge as long as the engine is designed for the most

knock-prone fuel to be expected with a given feedstock and process layout. The ξ-ε diagram can be a very useful tool for this purpose, since it facilitates the a priori estimation of the knock-tendency of syngas blends with regard to known fuels, such as methane and propane.
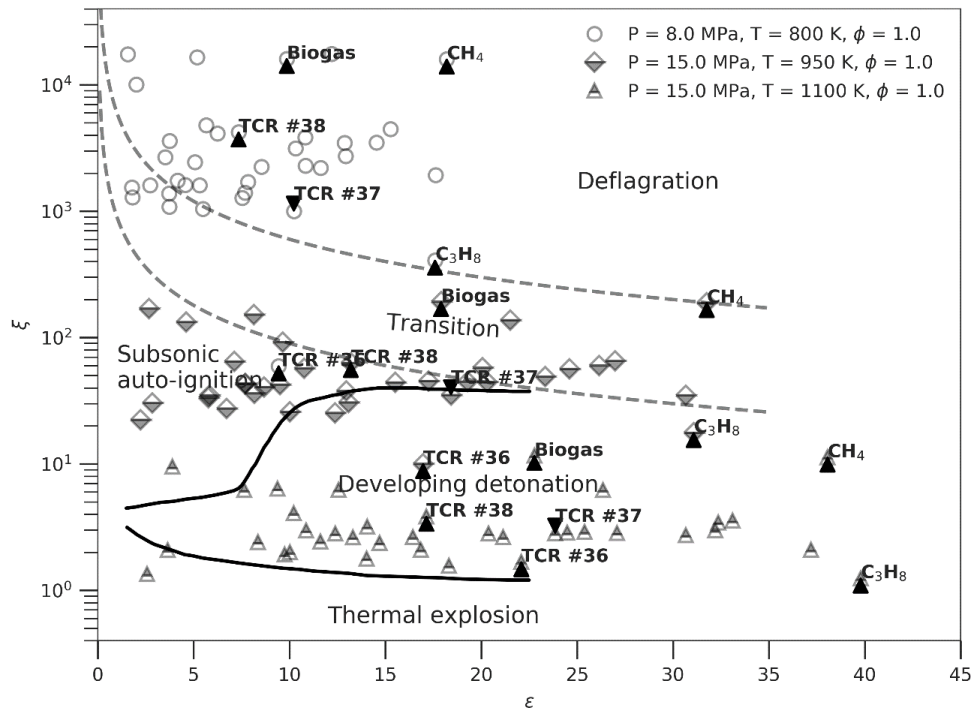

Figure 4: ξ-ε diagram at ϕ = 1.0
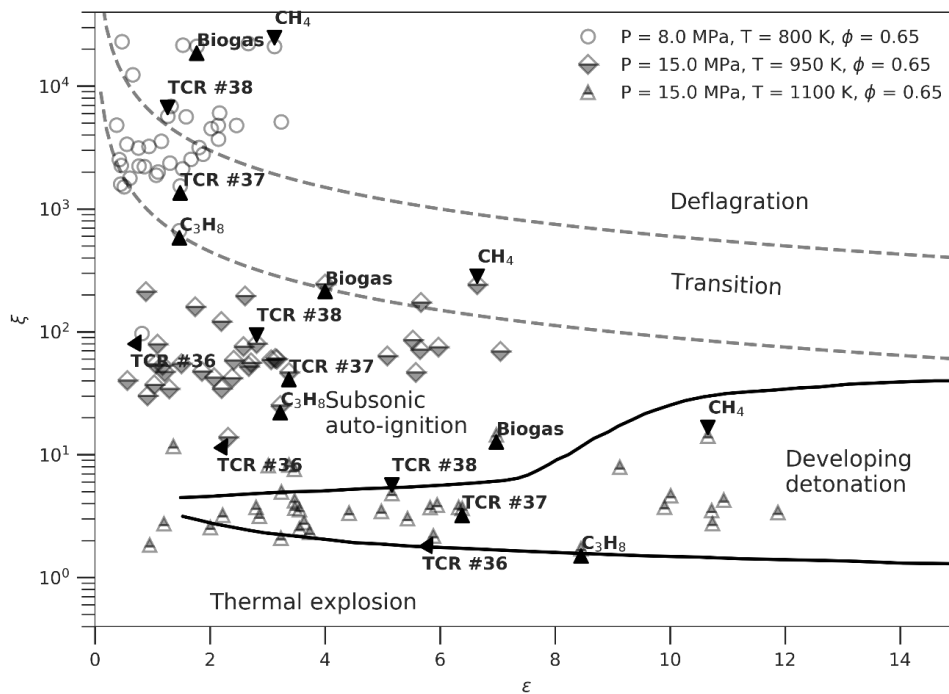

Figure 5: ξ-ε diagram at ϕ = 0.65

14

Effects of exhaust gas recirculation and water vapour

The effects of dilution with recirculated exhaust gas and water vapour were investigated for two representative fuel gases. Methane (fuel #32) was chosen as the reference fuel and compared to the syngas blend #5 which consists of 40 vol% H_2, 25 vol% CO, 15 vol% CH_4, 10 vol% CO_2 and 5 vol% of C_2H_4 and C_3H_8 respectively. In both cases, a stoichiometric base mixture was diluted with either H_2O or recirculated exhaust gas (EGR) from 0 to 40 vol%. The composition of the residual gas was modelled in detail assuming either chemical equilibrium or a frozen composition at 1 700 K. The frozen composition is expected to exhibit a higher reactivity due to dissociated species and radicals present in the mixture. The recirculated exhaust gases were assumed to be dry, since the effect of water vapour was investigated separately.

The results for a pressure of 15 MPa and a temperature of 950 K are displayed in the ξ-ε diagram presented in Figure 6. At these conditions, the undiluted fuel blend #5 is already in a regime of light knock at the upper limit of the detonation peninsula. Dilution with either recirculated exhaust gas or water vapour effectively decreases the values of ε, shifting the operating point towards the region above the narrow tip of the peninsula into safe conditions. It can be shown that the reduction of the ε-values is mainly due to an increase of the excitation times for the diluted mixtures. According to the detonation theory this reduces the amount of energy that can be transferred into the acoustic front of a pressure wave travelling through a hot spot. Thus, harmful detonations which result in engine knock are less likely to happen. In addition, there is also an increase in ignition delay times, but this only slightly increases the values of ξ and does not significantly contribute to the mitigation of knock-risk.

The results of this study confirm that mixtures diluted with residual gas or water vapour inherently exhibit less tendency to knock due to their auto-ignition characteristics. Of course, thermodynamic effects, such as an increase of the heat capacity ratio of the mixture by adding EGR or the cooling of the combustion system by injection of water, also play a role, but these effects are more obvious and we did not consider them here.

Considering equal volume fractions, water vapour has a much stronger anti-knock effect than dry exhaust gas, with fractions of only ≈ 10 vol% being sufficient to mitigate the risk of knock substantially. In practice, the recirculated exhaust gases will usually contain a certain amount of water vapour, depending on the type of system used (cooled or non-cooled EGR), which enhances their anti-knock effect. The difference between EGR at chemical equilibrium and at frozen conditions is primarily in the ξ-values. As expected, the frozen EGR composition shows a slightly higher reactivity. However, this does not significantly reduce its anti-knock capabilities and either the frozen or the equilibrium residual gas model can be used without altering the results with regard to the knock propensity.
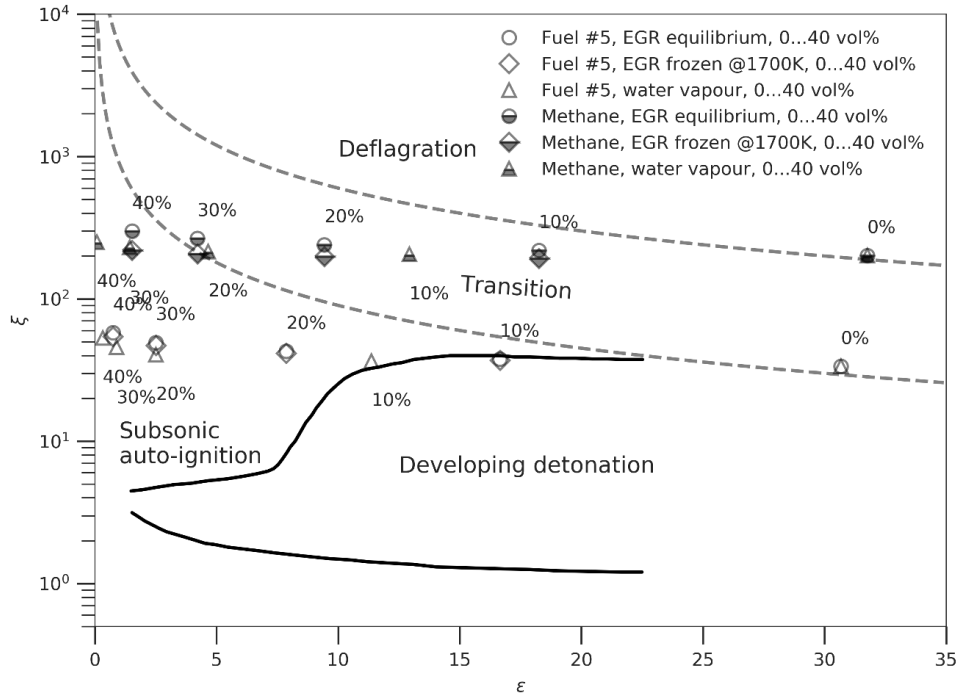
Figure 6: Effects of dilution with EGR and water vapour at *P* = 15 MPa, *T* = 950 K, *φ* = 1.0

4.   Conclusion

All investigated current knock index methods, including the classical methane number and new approaches such as the PKI propane knock index, showed to be not or only partly applicable to the syngas compositions expected in practical thermo-chemical conversion processes.

The critical compression ratio CR_c obtained from HCCI reactor simulations was proposed as alternative method for assessing the auto-ignition propensity of fuels in earlier studies. In the present study it could be confirmed that the simulated values of CR_c are linearly correlated to the corresponding methane numbers of the fuel, although with considerable scatter, which does not allow for a straightforward interpretation. Moreover, due to overlying thermodynamic effects the HCCI reactor simulation may provoke misleading results. Thus, its applicability as fuel rating tool is limited.

The *ξ-ε* diagram derived from the detonation theory was found to be a much more capable tool for prediction of the knock propensity of fuels. The required values for construction of the *ξ-ε* diagram can all be obtained from constant-volume chemical reaction kinetic simulations. Thus, the methodology has a great potential to be used for a priori characterisation of the auto-ignition propensity of fuels, without the need for experimentation. In *this study* the *ξ-ε* diagram was found to correctly reproduce the qualitative differences in knock-resistance of gaseous fuels such as methane, biogas, propane and syngas blends, as well as the increase of knock propensity due to the presence of higher hydrocarbons in the blend.

Lean equivalence ratios, exhaust gas recirculation and the addition of water vapour showed to be very effective measures for mitigating the risk of knock. In terms of the *ξ-ε* diagram, the anti-knock effect can be primarily attributed to an increase in excitation times which reduces the amount of energy that can be transferred into the acoustic front of an auto-ignition wave and leads to lower

values of ε. By contrast, the observed increase of ignition delay times due to dilution was found to have only a minor influence in this regard by slightly increasing the values of ξ.

The results of this study will still have to be validated experimentally, for example, by matching the ξ-ε diagram with real engine operating points from syngas-fuelled gas engines. It will also be necessary to extend the current limits of the detonation peninsula for fuels with very low excitation times and high values of ε, such as hydrogen. Since the excitation times can currently only be simulated, it is also of crucial importance to thoroughly assess the current kinetic schemes with regard to their capability of accurately reproducing the heat release profile in constant-volume reactor simulations.

Acknowledgements

References

[1] Wise DM. Investigation into producer gas utilisation in high performance natural gas engines [PhD thesis]. Fort Collins, Colorado: Colorado State University; 2013.

[2] Hiltner J, Hoops C, Wang P. Knock Prediction in Lean Burn Natural Gas Engines for Fuels with Significant Higher Hydrocarbon Content. In: WTZ Roßlau, editor. Proceedings 8th Dessau Gas Engine Conference. Dessau-Roßlau; 2013, p. 133–153.

[3] Zacharias F. Gasmotoren. 1st ed. Würzburg: Vogel; 2001.

[4] Gieseking B, Brown AS. Novel algorithm for calculating the methane number of liquefied natural gas with defined uncertainty. Fuel 2016;185:932–40. https://doi.org/10.1016/j.fuel.2016.07.105.

[5] van essen M, Gersen S, H J Van Dijk, G, Levinsky H. Next generation knock characterization. In: International Gas Union Research Conference 2014; 2014.

[6] Gersen S, van essen M, Levinsky H, van Dijk G. Characterizing Gaseous Fuels for Their Knock Resistance based on the Chemical and Physical Properties of the Fuel. SAE International Journal of Fuels and Lubricants 2016;9:1–13. https://doi.org/10.4271/2015-01-9077.

[7] van essen M, Gersen S. Ensure fitness for purpose for pipeline gas: Determine the quality of pipeline gas and secure safe and reliable use by calculating the Propane Knock Index (PKI) methane number. [June 06, 2019]; Available from: http://www.dnvgl.com/oilgas/natural-gas/fitness-for-purpose-for-pipeline-gas.html.

[8] Schultze M, Drexel C, Kollias-Pityrigkas G. Experimental and numerical investigation of gaseous hydrogenrich fuels in large gas engines. In: WTZ Roßlau, editor. Proceedings 10th Dessau Gas Engine Conference. Dessau-Roßlau; 2017, p. 307–318.

[9] Smith GP, Golden DM, Frenklach M, Moriarty NW, Eiteneer B, Goldenberg M et al. GRI-MECH 3.0. [March 08, 2017]; Available from: http://www.me.berkeley.edu/gri_mech/.

[10] Goodwin DG, Speth RL, Moffat HK, Weber BW. Cantera: An object-oriented software toolkit for chemical kinetics, thermodynamics, and Transport Processes. Zenodo; 2018.

[11] Gómez Montoya JP, Amell AA, Olsen DB. Prediction and measurement of the critical compression ratio and methane number for blends of biogas with methane, propane and hydrogen. Fuel 2016;186:168–75. https://doi.org/10.1016/j.fuel.2016.08.064.

[12] Bates L, Bradley D, Gorbatenko I, Tomlin AS. Computation of methane/air ignition delay and excitation times, using comprehensive and reduced chemical mechanisms and their relevance in engine autoignition. Combustion and Flame 2017;185:105–16. https://doi.org/10.1016/j.combustflame.2017.07.002.

[13] Bradley D, Kalghatgi GT. Influence of autoignition delay time characteristics of different fuels on pressure waves and knock in reciprocating engines. Combustion and Flame 2009;156(12):2307–18. https://doi.org/10.1016/j.combustflame.2009.08.003.

[14] Netzer C, Seidel L, Pasternak M, Lehtiniemi H, Perlman C, Ravet, Frédéric, Mauss, Fabian. Three-dimensional computational fluid dynamics engine knock prediction and evaluation based on detailed chemistry and detonation theory. International Journal of Engine Research 2018;19(1):33–44.

[15] Gu XJ, Emerson DR, Bradley D. Modes of reaction front propagation from hot spots. Combustion and Flame 2003;133(1-2):63–74. https://doi.org/10.1016/S0010-2180(02)00541-2.

[16] Conti R, Jäger N, Neumann J, Apfelbacher A, Daschner R, Hornung A. Thermocatalytic Reforming of Biomass Waste Streams. Energy Technol. 2017;5(1):104–10. https://doi.org/10.1002/ente.201600168.

[17] Neumann J, Meyer J, Ouadi M, Apfelbacher A, Binder S, Hornung A. The conversion of anaerobic digestion waste into biofuels via a novel Thermo-Catalytic Reforming process. Waste Manag 2016;47(Pt A):141–8. https://doi.org/10.1016/j.wasman.2015.07.001.

[18] Jäger N, Conti R, Neumann J, Apfelbacher A, Daschner R, Binder S et al. Thermo-Catalytic Reforming of Woody Biomass. Energy Fuels 2016;30(10):7923–9. https://doi.org/10.1021/acs.energyfuels.6b00911.

[19] Mahmood ASN, Brammer JG, Hornung A, Steele A, Poulston S. The intermediate pyrolysis and catalytic steam reforming of Brewers spent grain. Journal of Analytical and Applied Pyrolysis 2013;103:328–42. https://doi.org/10.1016/j.jaap.2012.09.009.

[20] Ouadi M, Brammer JG, Yang Y, Hornung A, Kay M. The intermediate pyrolysis of de-inking sludge to produce a sustainable liquid fuel. Journal of Analytical and Applied Pyrolysis 2013;102:24–32. https://doi.org/10.1016/j.jaap.2013.04.007.

[21] Yang Y, Brammer JG, Mahmood ASN, Hornung A. Intermediate pyrolysis of biomass energy pellets for producing sustainable liquid, gaseous and solid fuels. Bioresour Technol 2014;169:794–9. https://doi.org/10.1016/j.biortech.2014.07.044.

[22] Neumann J, Binder S, Apfelbacher A, Gasson JR, Ramírez García P, Hornung A. Production and characterization of a new quality pyrolysis oil, char and syngas from digestate – Introducing the thermo-catalytic reforming process. Journal of Analytical and Applied Pyrolysis 2015;113:137–42. https://doi.org/10.1016/j.jaap.2014.11.022.

[23] Neumann J, Jäger N, Apfelbacher A, Daschner R, Binder S, Hornung A. Upgraded biofuel from residue biomass by Thermo-Catalytic Reforming and hydrodeoxygenation. Biomass and Bioenergy 2016;89:91–7. https://doi.org/10.1016/j.biombioe.2016.03.002.

[24] European Association of Internal Combustion Engine Manufacturers. MWM MN calculation program; 2017.

[25] Cummins Westport. Fuel Quality Calculator. [June 06, 2019]; Available from: http://www.cumminswestport.com/fuel-quality-calculator.

[26] Wang Z, Liu H, Reitz RD. Knocking combustion in spark-ignition engines. Progress in Energy and Combustion Science 2017;61:78–112. https://doi.org/10.1016/j.pecs.2017.03.004.

[27] Bates L, Bradley D, Paczko G, Peters N. Engine hot spots: Modes of auto-ignition and reaction propagation. Combustion and Flame 2016;166:80–5. https://doi.org/10.1016/j.combustflame.2016.01.002.

[28] Ranzi E, Frassoldati A, Grana R, Cuoci A, Faravelli T, Kelley AP et al. Hierarchical and comparative kinetic modeling of laminar flame speeds of hydrocarbon and oxygenated fuels. Progress in Energy and Combustion Science 2012;38(4):468–501. https://doi.org/10.1016/j.pecs.2012.03.004.

[29] Bates L. Characterisation of reaction propagation from auto-ignition [PhD thesis]. Leeds: University of Leeds; 2016.